# Forces between Two Glass Surfaces with Adsorbed Hexadecyltrimethylammonium Salicylate

Toyoko Imae,*[,†,‡] Motohisa Kato,[‡] and Mark Rutland[§,||]

*Research Center for Materials Science and Graduate School of Science, Nagoya University, Chikusa, Nagoya 464-8602, Japan, and School of Chemistry, University of Sydney, Sydney, New South Wales 2006, Australia*

*Received June 24, 1999. In Final Form: October 29, 1999*

Forces have been measured for hexadecyltrimethylammonium salicylate ($C_{16}$TASal) layers on glass beads. During the inward process, hydrophobic attraction occurred at lower adsorption of $C_{16}$TASal and electrostatic repulsion interactions happened at higher adsorption. While the jump-in phenomenon was observed for solutions of concentrations below the critical micelle concentration (cmc = 0.15 mM), the step-in phenomenon was characteristic for solutions at the cmc and above the cmc, suggesting the push-out of adsorbed $C_{16}$TASal layers and/or inserted micelles. The remarkable pull-off phenomenon on the outward process occurred for all solutions, indicating a strong interaction between $C_{16}$TASal molecules. For aqueous 0.15 mM $C_{16}$TASal solutions of various NaSal concentrations, on the inward process, the electrostatic repulsive interaction decreased with adding NaSal. This is due to the electrostatic shielding by salt excess. The height of the force wall on the inward process reached a maximum at 0.01 M NaSal, but the interlocking between molecules on two surfaces during the outward process was minimized at 0.1 M NaSal. These tendencies, which are different from that of the electrostatic repulsion interaction, imply the strong cohesion between adsorbed $C_{16}$TASal layers.

## Introduction

Cationic surfactants with aromatic counterions such as alkyltrimethylammonium and alkyltrimethylpyridinium salicylates display remarkable rheological behavior, such as spinnability and viscoelasticity in aqueous solutions.[1−5] The characteristic behavior results from the fact that rodlike micelles entangle and contact each other to form a three-dimensional pseudonetwork, although the behavior is not observed in aqueous solutions of entangled rodlike micelles of cationic surfactants with halide counterions.[5,6] Then the specific adsorption and penetration ability of salicylate counterions are related to the solution behavior and the micellar growth.[7] Thus it is necessary to elucidate the electrical structure of micelles and the interaction forces between micelles.

Imae et al.[3,4,8,9] have reported size, electrophoretic mobility, and rheological behavior of tetradecyl- and hexadecyltrimethylammonium salicylate ($C_{14}$TASal, $C_{16}$TASal) micelles in aqueous media. While the length of rodlike micelles increases with increasing sodium salicylate (NaSal) concentration up to 0.1 M, further addition of NaSal diminishes the micellar size to be spherical at 1 M NaSal. The spinnable, viscoelastic behavior of the solutions depends on micellar size and shape.[3,4] The net surface charge of micelles converts the sign from positive to negative through neutral at about 0.1 M NaSal.[8,9] This shows that the micellar size and the solution behavior are dominated by the specific adsorption and penetration of salicylate ions.

Cassidy and Warr[10] have determined surface potentials of mixtures of $C_{14}$TABr and NaSal in water by the titration of a micelle-bound indicator and found the strong binding of salicylate ion which lowers effectively the surface potential of the micelles. On the other hand, the zeta potentials calculated from electrophoretic mobility by using the Smoluchowski equation[11] are lower than the electrostatic potentials at the micellar surface. Cassidy and Warr[10] have proposed the model where the adsorption sites in micelles continuously vary from the exterior surface binding salicylate to the hydrophobic core intercalating salicylate.

The electrostatic potential as well as the other interaction potentials can also be determined by the force measurement between two surfaces which adsorb molecules or are covered by them. At present, the Israelachvili[12] and Parker[11] surface force apparatuses and the force microscopy[13] are available for measurement and analysis of surface interactions and forces. The force measurement between surfaces covered by $C_{16}$TASal layers should give us more detailed consideration of the interactions within and between micelles and their origin. In the present work, the measurement is performed between glass beads which

* To whom all correspondence should be addressed. Tel.: 81-52-789-5911. Fax: 81-52-789-5912. E-mail: imae@chem2.chem.nagoya-u.ac.jp.

† Research Center for Materials Science, Nagoya University.

‡ Graduate School of Science, Nagoya University.

§ University of Sydney.

|| Current address: Surface Chemistry, Royal Institute of Technology, 100 44 Stockholm, Sweden, and Institute for Surface Chemistry, Box 5607, 114 86 Stockholm, Sweden.

(1) Gravsholt, S. *J. Colloid Interface Sci.* **1976**, *57*, 575.

(2) Rehage, H.; Hoffmann, H. *Faraday Discuss. Chem. Soc.* **1983**, *76*, 363.

(3) Imae, T.; Hashimoto, K.; Ikeda, S. *Colloid Polym. Sci.* **1990**, *268*, 460.

(4) Hashimoto, K.; Imae, T.; Nakazawa, K. *Colloid Polym. Sci.* **1992**, *270*, 249.

(5) Imae, T. In *Structure and Flow in Surfactant Solutions*; Herb, C. A., Prud'homme, R. K., Eds.; ACS Symposium Series 578; American Chemical Society: Washington, DC, 1994; p 140.

(6) Claussen, T. M.; Vinson, P. K.; Minter, J. R.; Davis, H. T.; Yalmon, Y.; Miller, W. G. *J. Phys. Chem.* **1992**, *96*, 474.

(7) Olsson, U.; Soderman, O.; Guering, P. *J. Phys. Chem.* **1986**, *90*, 5223.

(8) Imae, T. *J. Phys. Chem.* **1990**, *94*, 5953.

(9) Imae, T.; Kohsaka, T. *J. Phys. Chem.* **1992**, *96*, 10030.

(10) Cassidy, M. A.; Warr, G. G. *J. Phys. Chem.* **1996**, *100*, 3237.

(11) Parker, J. L. *Langmuir* **1992**, *8*, 551.

(12) Israelachvili, J. N. *Intermolecular and Surface Forces*, 2nd ed.; Academic Press: New York, 1992.

(13) Ducker, W. A.; Senden, T. J.; Pashley, R. M. *Langmuir* **1992**, *8*, 1831.

10.1021/la990824y CCC: $19.00 
Published on Web 01/04/2000

are immersed in aqueous solutions of various $C_{16}$TASal concentrations below and above the critical micelle concentration $C_0$ (cmc = 0.15 mM) and of different NaSal concentrations. The force measurements have been reported for aqueous solutions of cationic surfactants with halide counterions,[14−22] but no measurements have been made for surfactants with salicylate counterion. The influence of counterion species is discussed.

## Experimental Section

Synthesis of $C_{16}$TASal has been described previously.[3−5] The NaSal used was of commercial grade. Water was redistilled from alkaline $KMnO_4$.

The measurement and analysis of surface interactions and forces (MASIF, Anutech Pty Ltd.) apparatus, based on the development by Parker,[11] was used for the surface force measurement. Two surfaces were mounted at the ends of the piezoelectric tube and the bimorph force sensor, respectively. The bimorph enclosed in a Teflon sheath was clamped to a solution chamber. The piezoelectric motion from a linear variable displacement transducer (LVDT) and the signal from the bimorph charge amplifier were recorded in response to the motor translation of the piezoelectric tube during the course of inward and outward force runs.

The surfaces were pushed together until contact. Then the motion of the piezoelectric tube was transmitted directly to the bimorph sensor. The resulting straight line was used to calculate the deflection of the bimorph signal using the displacement/LVDT calibration constant of 0.526 $\mu$m/V which was determined by interferometry. The force $F$ in the surface force region was then obtained by multiplying the deflection by the spring constant (∼200 N/m), which was determined by the weight method. The glass surfaces were prepared by melting the end of a 1.5 mm glass rod in gas burner until a molten droplet of glass is formed. The radius (∼1.2 mm) of droplet was measured by a micrometer. Then the force $F$ scaled by the effective radius of curvature ($R = D_1D_2/(D_1 + D_2)$ for diameters $D_1$ and $D_2$ of two glass beads) was plotted as a function of separation, which was evaluated as the difference of deflections in the force region and in contact.

## Results

For aqueous $C_{16}$TASal solutions of various $C_{16}$TASal concentrations without NaSal, the force curves on the inward process are plotted in Figure 1 as a function of separation. While the weak repulsive interaction occurred between two glass surfaces in water without $C_{16}$TASal, and the attraction was observed in a 0.01 mM $C_{16}$TASal solution, the repulsive force was again generated at $C_{16}$-TASal concentrations above 0.01 mM. At the shorter intersurface separation in 0.01 and 0.05 mM solutions, the surfaces jumped into an adhesive contact at 7 and 9 nm separations, respectively. On the other hand, the steep increase of the repulsive force was observed at 4−5 nm separation for a 0.15 mM solution and at 8−9 nm separation for a 0.3 mM solution. The push-out occurred at one step (32−35 mN/m) for the 0.15 mM solution and at two steps (first at 21−40 mN/m and second at 40−42 mN/m) for the 0.3 mM solution. The positions of steps were marked in Figure 1.

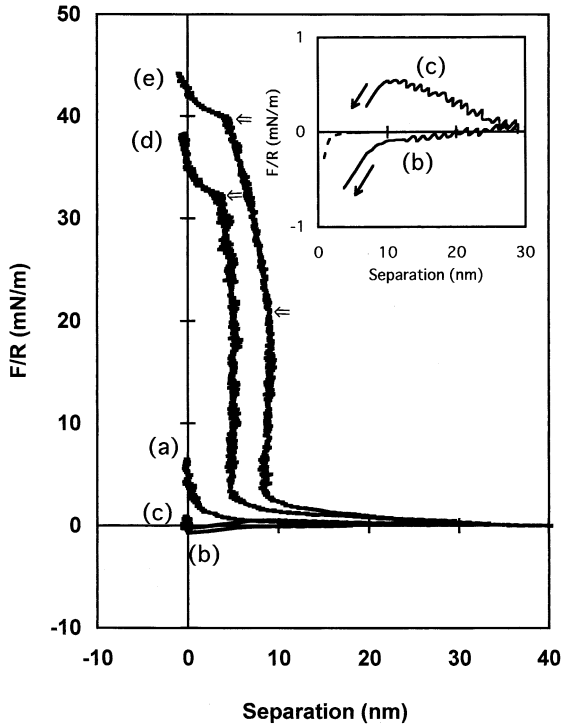


**Figure 1.** Force versus separation curves, on the inward process, between glass surfaces immersed in $C_{16}$TASal solutions. $C_{16}$TASal concentration (mM): (a) 0; (b) 0.01; (c) 0.05; (d) 0.15; (e) 0.3. The inserted figure represents the force versus separation for 0.01 mM (b) and 0.05 mM (c) $C_{16}$TASal solutions and the calculated van der Waals attration at a Hamaker constant of $0.8 \times 10^{-20}$ J. Arrows represent the starting point of push-out steps.

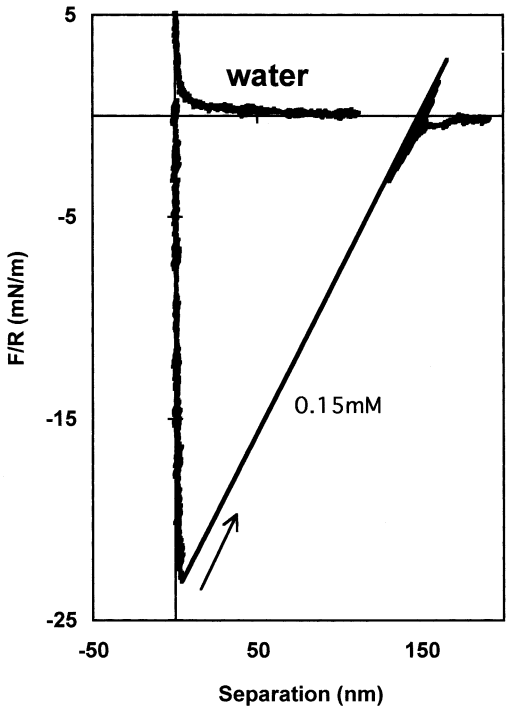


**Figure 2.** Force versus separation curves, on the outward process, between glass surfaces immersed in water and a 0.15 mM $C_{16}$TASal solution.

The interesting results were obtained on the outward process where two surfaces in contact are pulled apart. Figure 2 shows the force curves on the outward process between glass surfaces immersed in water without $C_{16}$-TASal and in 0.15 mM $C_{16}$TASal solution. While the force

(14) Parker, J. L.; Yaminsky, V. V.; Claesson, P. M. *J. Phys. Chem.* **1993**, *97*, 7706.
(15) Parker, J. L.; Rutland, M. W. *Langmuir* **1993**, *9*, 1965.
(16) Rutland, M. W.; Parker, J. L. *Langmuir* **1994**, *10*, 1110.
(17) Drummond, C. J.; Senden, T. J. *Colloids Surf., A*: *Phys. Eng. Aspects* **1994**, *87*, 217.
(18) Johnson, S. B., Drummond, C. J., Scales, P. J. Nishimura, S. *Colloids Surf., A*: *Phys. Eng. Aspects* **1995**, *103*, 195.
(19) Craig, V. S. J. *J. Colloid Interface Sci.* **1996**, *183*, 260.
(20) Yaminsky, V. V.; Ninham, B. W.; Stewart, A. M. *Langmuir* **1996**, *12*, 836.
(21) Yaminsky, V. V.; Jones, C.; Yaminsky, F.; Ninham, B. W. *Langmuir* **1996**, *12*, 1936.
(22) Hu, K.; Bard, A. J. *Langmuir* **1997**, *13*, 5418.

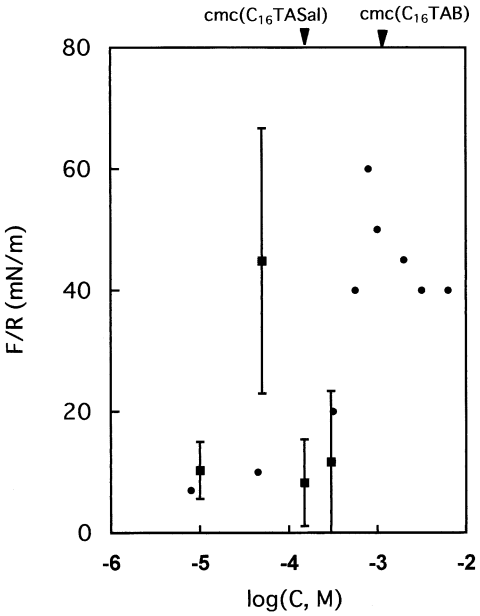


**Figure 3.** Adhesion forces as a function of surfactant concentration: ■, $C_{16}$TASal; ●, $C_{16}$TAB (ref 16). Bars represent the standard deviations.

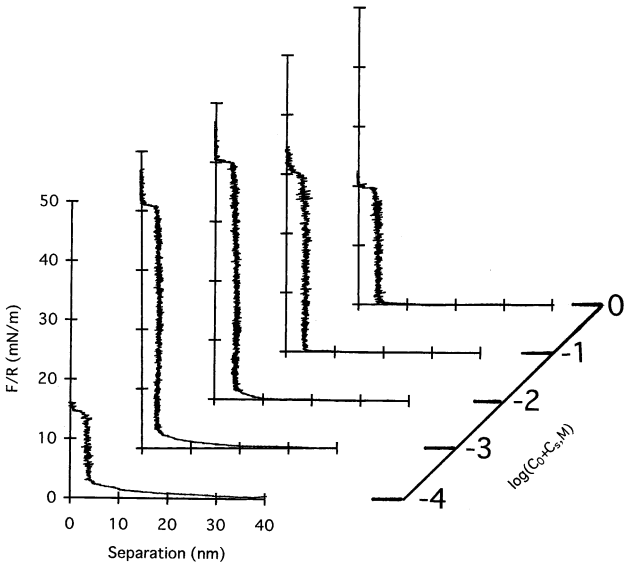


**Figure 4.** Force versus separation curves, on the inward process, between glass surfaces immersed in 0.15 mM $C_{16}$TASal solutions at various NaSal concentrations (0−1.0 M).

curve on the outward process in water turned back the same way as for the inward process, the strong pull-off phenomenon was observed in the 0.15 mM solution and in other $C_{16}$TASal solutions examined. The adhesion forces to be equivalent to the pull-off force are plotted in Figure 3 as a function of $C_{16}$TASal concentration $C$ (M). The strongest interlocking was found at the 0.05 mM solution.

Figure 4 shows the force versus separation curves, on the inward process, between glass surfaces immersed in aqueous solutions of various NaSal concentrations at 0.15 mM $C_{16}$TASal concentration. While the repulsive interaction occurred at longer separation for a solution without NaSal, it decreased with adding NaSal. The push-out phenomenon was the common profile for all solutions. The push-out occurred at a distance of 3−5 nm and surface pressure of 20−40 mN/m, depending on NaSal concentration. Figure 5 shows the force-wall height as a function of ionic strength ($C_0 + C_s$), where $C_s$ (M) is NaSal concentration. The height reached a maximum at the ionic

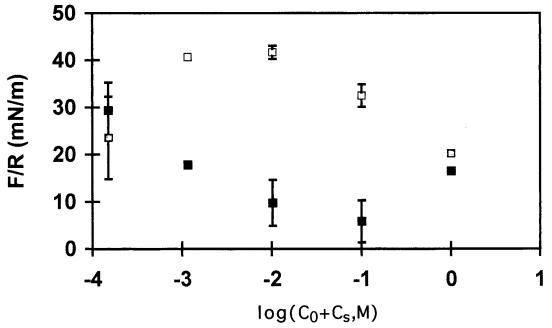


**Figure 5.** Force-wall heights (□) and adhesion forces (■) as a function of ionic strength between glass surfaces immersed in 0.15 mM $C_{16}$TASal solutions. Bars represent the standard deviations.

strength of 0.01 M. The strong adhesion occurred on the outward process for all solutions examined. As shown in Figure 5, the interlocking decreased with increasing NaSal concentration and increased at the ionic strength above 0.1 M.

## Discussion

The interaction force $F = -(\partial V_{ss}/\partial H)_{T,P}$ between two spheres separated by the separation $H$ is related to the interaction potential energy $V_{pp}$ per unit area between two flat planar surfaces, under the Derjaguin approximation,[23] by

$$F/R = \pi V_{pp} \tag{1}$$

if the separation between the surfaces is markedly smaller than the radii of spheres. $V_{ss}$ is the interaction potential between two sphere surfaces. The interaction potential between glass surfaces with adsorbed $C_{16}$TASal is described as a sum of the electrostatic repulsion potential $V_{elec}$, the hydration repulsion potential $V_{hydr}$, the steric repulsion potential $V_{steric}$, the London−van der Waals attraction potential $V_{vdw}$, and the hydrophobic attraction potential $V_{hbic}$, that is

$$V = V_{elec} + V_{hydr} + V_{steric} + V_{vdw} + V_{hbic} \tag{2}$$

The interaction forces between two silica surfaces immersed in aqueous NaCl solutions have been observed in the Israelachvili surface force apparatus and the force microscope.[13−15,24−26] Ducker et al.[13] have measured, by using the force microscope, the surface force between a silica-glass sphere and a flat oxidated silicon wafer in an aqueous NaCl solution. At smaller separations, no adhesive minimum or no van der Waals attraction dominates, but the force is greater than that predicted from the DLVO theory by using an exact numerical solution to the Poisson−Boltzmann equation and a Hamaker constant of $0.8 \times 10^{-20}$ J. A similar deviation from the theoretical calculation is also obtained in the force curve from the Parker surface force apparatus between two glass beads in water in the present work. The possible explanation of this additional short-range repulsive effect described by Horn et al.,[24] Parker et al.,[14,15] and Rutland[25] is the contribution of hydration repulsion. This indicates that water adjacent to the silica surface is not equivalent to bulk water. Ducker et al.[13] suggest the existence of a gel layer on the surface of silica and a shift in the position of

(23) Derjaguin, B. V. *Kolloid-Z.* **1934**, *69*, 155.
(24) Horn, R. G.; Smith, D. T.; Haller, W. *Chem. Phys. Lett.* **1989**, *162*, 404.
(25) Rutland, M. W. *Colloids Surf., A: Phys. Eng. Aspects* **1994**, *83*, 121.

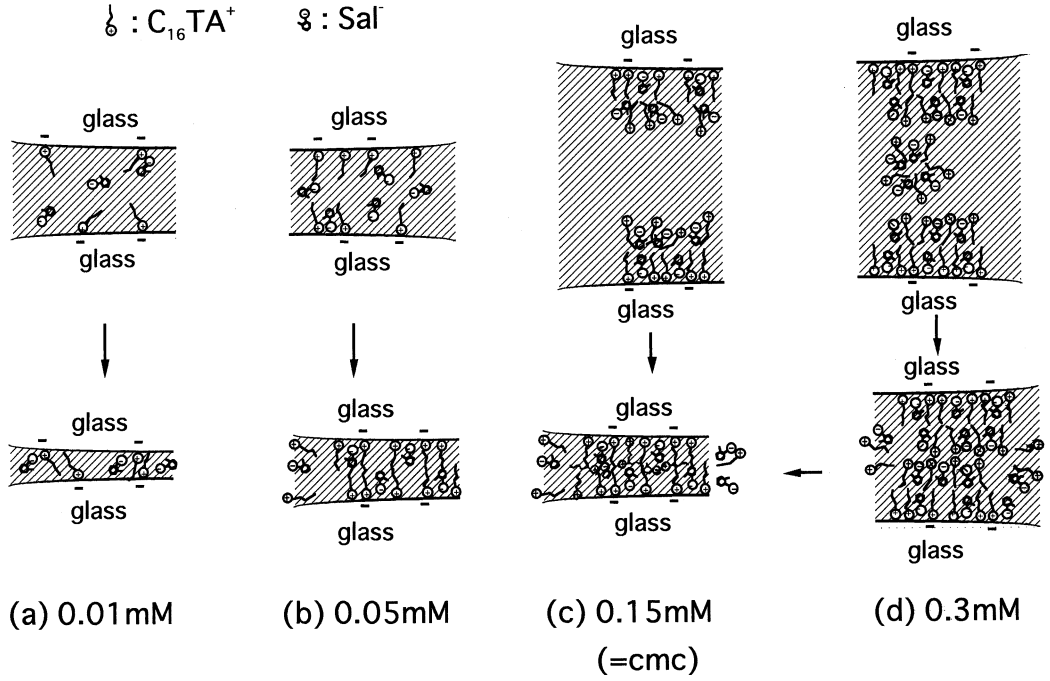


**Figure 6.** Adsorption model of $C_{16}$TASal on glass surfaces immersed in $C_{16}$TASal solutions.

the surface charge plane besides the hydration of silica. According to Vigil et al.,[26] the repulsion may be a steric/entropic one originating from the surface-located polysilicates. Larson et al.[27] have supported Vigil's explanation.

In a $C_{16}$TASal solution without NaSal, the interaction force is always attractive at a 0.01 mM $C_{16}$TASal concentration, which is far below the cmc. Since the isoelectric point of silica is around pH 3, glass surfaces are negatively charged in the solutions examined in the present work. Then the electrostatic adsorption of hexadecyltrimethylammonium ($C_{16}$TA) ions occurs on the $SiO^-$ centers of glass. The adsorption model is represented in Figure 6. As seen in the inset of Figure 1, the force curve for the 0.01 mM $C_{16}$TASal solution is more attractive than the van der Waals potential calculated with a Hamaker constant of $0.8 \times 10^{-20}$ J.[13] Therefore, the attraction may include the hydrophobic interaction besides the van der Waals effect. The observation of the long-range attractive force stronger than expected for the van der Waals attraction has been reported between hydrophobic silanated glass surfaces,[28] between neutral deposited monolayers of double-chain cationic surfactants,[29,30] and between adsorbed layers of hexadecyltrimethylammonium bromide ($C_{16}$TAB) on glass and silica surfaces.[14,31] The additional force is described by an exponential attraction $F/R = -a \exp(-H/b)$ with constants $a$ and $b$ for the forces between silanated glass surfaces in water.[28] When the exponential equation is applied to the force curve at 0.01 mM $C_{16}$TASal concentration in Figure 1 in the present work, the values of $a = 2.4$ and $b = 3.0$ are the best fit to the observed force curve. The values are close to those ($a = 3.2$, $b = 5.6$) reported by Parker and Claesson.[28]

**Table 1. Debye−Hückel Parameter and Electrostatic Potential of Glass Surfaces in Aqueous $C_{16}$TASal Solutions with and without NaSal**

| $C$, mM | $C_s$, M | $\kappa^{-1}$, nm | $\psi$, mV |
|---|---|---|---|
| 0 | 0 | 30 | −77 |
| 0.05 | | 43 | 111 |
| 0.15 | | 10−25 | 163−177 |
| 0.3 | | 18−50 | 136−149 |
| 0.15 | $10^{-3}$ | 9.0−25 | 72−88 |
| | $10^{-2}$ | 3.0−4.0 | 32−66 |
| | $10^{-1}$ | 0.96−10 | 12−22 |
| | 1 | 0.30−6.7 | −18−24 |

At the short separation below 7 nm on the force curve at the 0.01 mM $C_{16}$TASal solution, the surfaces are pulled into the adhesion by the apparent attractive interaction. The same phenomenon is observed for $C_{16}$TAB on glass and mica.[14] Parsegian and Podgornik[32] have argued that this apparent attraction may be due to a sudden reduction of the repulsive double-layer interaction. However, Parker et al.[14] insist that the experimental results are not necessarily consistent with the model. The reason may be that the presence of adsorbed surfactants on surfaces renders the surface partially hydrophobic, and the resulting high intersurface tension against water leads to adhesion.[15]

The apparent attractive interaction pulls surfaces into the adhesion at the short separation in the force curve for a 0.05 mM $C_{16}$TASal solution, as well as for a 0.01 mM $C_{16}$TASal. On the other hand, the force at the long-range distance is electrostatically repulsive because of the excess adsorption of cationic surfactant. The electrostatic repulsion is also observed at the long-range distance for 0.15 and 0.30 mM $C_{16}$TASal solutions. The Debye−Hückel parameter $\kappa$ and the electrostatic potential $\psi$ are calculated on the basis of the DLVO theory[33] and listed in Table 1, where the data for water without $C_{16}$TASal are also

(26) Vigil, G.; Xu, Z.; Steinberg, S.; Israelachvili, J. N. *J. Colloid Interface Sci.* **1994**, *165*, 367.
(27) Larson, I.; Drummond, C. J.; Chan, D. Y. C.; Grieser, F. *J. Phys. Chem.* **1995**, *99*, 2114.
(28) Parker, J. L.; Claesson, P. M. *Langmuir* **1994**, *10*, 635.
(29) Claesson, P. M.; Christenson, H. K. *J. Phys. Chem.* **1988**, *92*, 1650.
(30) Tsao, Y.; Yang, S. X.; Evans, D. F.; Wennerström, H. *Langmuir* **1991**, *7*, 3154.
(31) Craig, V. S. J.; Ninham, B. W.; Pashley, R. M. *Langmuir* **1999**, *15*, 1562.
(32) Podgornik, R.; Parsegian, V. A. *J. Chem. Phys.* **1991**, *154*, 477.
(33) Hunter, R. J. *Foundations of Colloid Science*; Oxford University Press: New York, 1989; Vol. 1, Chapter 7.

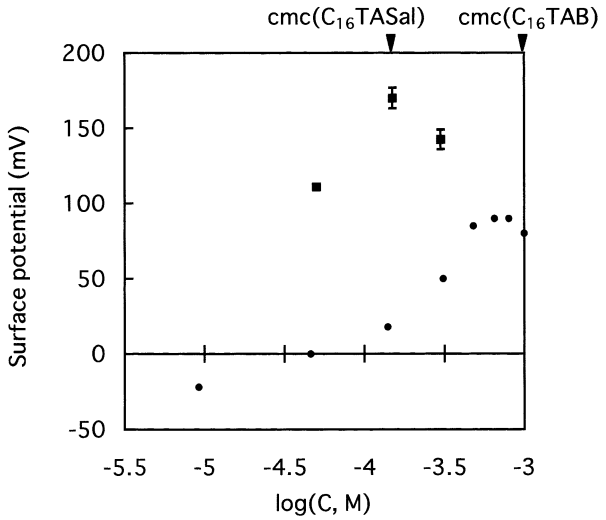


**Figure 7.** Surface potentials calculated from the force curves as a function of surfactant concentration: ■, $C_{16}$TASal; ●, $C_{16}$TAB (ref 16). Bars represent the standard deviations.

included. The surface potentials are plotted as a function of $C_{16}$TASal concentration in Figure 7. The surface potentials for aqueous $C_{16}$TAB solutions calculated from the force curves by the Parker surface force apparatus[14,16] are also included. The surface potentials increase with increasing surfactant concentration up to the cmc, suggesting the increase in the excess adsorption of cationic surfactants on glass surfaces. It may be noted that the surface potential at the cmc is larger for $C_{16}$TASal than for $C_{16}$TAB. It indicates that the adsorption equilibrium on glass surfaces depends on cmc and counterions, and the maximum surface coverage of $C_{16}$TASal is larger than that of $C_{16}$TAB.

The characteristic profile for $C_{16}$TASal solutions at cmc and higher concentration is the step-in phenomenon. The step-in distances of 4−5 nm for a 0.15 mM solution and 8−9 nm for a 0.30 mM solution correspond to two- and four-layer separations, respectively. As illustrated in Figure 6, bilayers of $C_{16}$TASal are adsorbed on each glass surface at the cmc and micelles are placed between them at concentration above the cmc. On the inward process at the cmc, each monolayer within adsorbed bilayers is pushed out. On the other hand, at concentration above the cmc, collapsed micelles are pushed out and, in turn, each adsorbed monolayer is pushed out. The remarkable step-in phenomenon is reported for $C_{16}$TAB adsorbed layers on glass surfaces[16] and for hexadecylpyridinium chloride ($C_{16}$PC) adsorbed layers on silica surfaces.[19] Their step-in distances are equivalent to the push-out of each monolayer adsorbed on a surface, as well as the push-out of the $C_{16}$TASal system at the cmc in the present work. However, their force-wall heights are far below that of the $C_{16}$TASal system. This indicates the stronger and more compact adsorption of $C_{16}$TASal than of $C_{16}$TAB on surfaces.

Rennie et al.[34] have reported the result of specular neutron reflection in order to study the structure of a $C_{16}$TAB layer adsorbed at the interface between an amorphous silica plate and a solution. They favorably support the structure of a defective bilayer at concentrations of $^1/_3$ and $^2/_3$ the cmc (0.9 mM). Then the structure of $C_{16}$TASal layers can be a less defective bilayer at the corresponding concentrations, as illustrated in Figure 6.

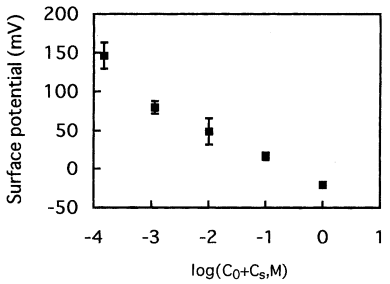


**Figure 8.** Surface potentials calculated from the force curves of $C_{16}$TASal as a function of ionic strength. Bars represent the standard deviations.

On the pull-off process where two surfaces in contact are pulled apart, the jump-out process of surfaces is observed even at the 0.01 mM $C_{16}$TASal solution. Since the adhesion increases with adsorbing $C_{16}$TASal at concentrations below the cmc, as seen in Figure 3, it is interpreted that the adhesion is due to adsorption of surfactant in a narrow gap around the contact area and is induced by the favorable interaction of hydrophobic tails across the gap.[16] At the cmc and above the cmc, the adhesion decreases. After the push-out process, residual $C_{16}$TASal molecules are caught between $C_{16}$TASal layers adsorbed on both surfaces, as illustrated in Figure 6. Such trapped molecules act to disturb the hydrophobic interactions between $C_{16}$TASal layers, different from the case below the cmc.

It must be noticed that a large experimental error appears in the determination of adhesion forces because of the worse reproducibility and time dependence of the molecular arrangement in a gap. The time dependence of adhesion forces has been reported by Parker and Rutland.[15] In the present work, measurement time of adhesion is about 30−40 s after contact. The interlocking by $C_{16}$TASal adsorption is of the same order as those of $C_{16}$TAB[14,16,35] and $C_{16}$PC[19] on silica surfaces, as seen in Figure 3. This is consistent with the interpretation that the interlocking results from the hydrophobic interaction, as described above, being independent of the counterions.

The electrostatic repulsion force is decreased, when NaSal is added in aqueous $C_{16}$TASal solutions, as shown in Figure 4. The calculated surface potentials are listed in Table 1 and plotted as a function of ionic strength in Figure 8. The gradual decrease of surface potentials with increasing ionic strength is similar to that of ζ potentials of $C_{16}$TASal micelles in solutions.[8] However, ζ potentials calculated from the electrophoretic mobilities are smaller than the surface potentials obtained in the present work.

The interaction between cationic surfactant and NaSal has been investigated on surfaces of silica particles by Favoriti et al.[35] They reported that, at the high solution pH above the silica isoelectric point, salicylate ions are repelled from the inner layer in the double layer structure of adsorbed $C_{16}$PC, owing to the high negative surface charge density on the silica particles. This situation occurs even for $C_{16}$TASal layers on glass beads in the present work. Then the surface potentials on glass beads are higher than the ζ potentials of $C_{16}$TASal micelles in solutions.

The size, shape, and electric properties have been investigated for $C_{14}$TASal and $C_{16}$TASal micelles in solutions with NaSal.[8,9] Although the length of rodlike micelles increases with increasing NaSal concentration up to 0.1 M NaSal, the size diminishes toward spherical micelles with further increase of NaSal. Then the micellar

(34) Rennie, A. R.; Lee, E. M.; Simister, E. A.; Thomas, R. K. *Langmuir* **1990**, *6*, 1031.

(35) Favoriti, P.; Mannebach, M. H.; Treiner, C. *Langmuir* **1996**, *12*, 4691.

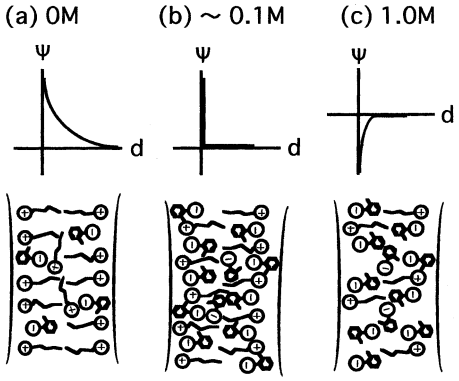


**Figure 9.** Schematic representation of adsorption models at different ionic strengths.

charge is changed from positive to negative at 0.1 M NaSal. This behavior results from the shielding of electrostatic repulsion between cationic surfactants in micelles and the excess penetration of salicylate ions in micelles. The shielding of electrostatic repulsion induces the more compact arrangement of surfactant molecules in micelles and in adsorbed layers on glass beads. This is consistent with the fact that the force-wall by the adsorbed layers on glass beads heightens with increasing ionic strength (see Figure 5). However, at high NaSal, excess salicylate ions penetrate into hydrophobic regions of cationic surfactant layers on glass beads. Then the hydrophobic interaction between surfactants is suppressed and, therefore, the force-wall height is decreased.

The adhesion force is related to the hydrophobic interaction and is strong for a more compact arrangement of surfactant molecules. However, at high ionic strengths up to 0.1 M NaSal, excess NaSal molecules get between surfactant layers on glass beads contacting, resulting in the decrease of adhesion force, as seen in Figure 5. On the other hand, at 1 M NaSal, excess salicylate ions adsorb on glass beads rather than between surfactant layers. Then the adhesion force at 1 M NaSal is higher than that at 0.1 M NaSal. The adsorption models at different ionic strengths are schematically represented in Figure 9.

## Conclusions

Force measurements have been carried out between $C_{16}$TASal layers adsorbed on glass beads from aqueous solutions. During the inward process, the hydrophobic attraction interaction occurred at lower adsorption of $C_{16}$-TASal, and the electrostatic repulsion interaction was observed for aqueous $C_{16}$TASal solutions of concentrations above 0.01 mM. The jump-in phenomenon was observed at 7−9 nm separation for solutions of concentrations below the cmc. The characteristic profile for aqueous $C_{16}$TASal solutions of cmc and higher concentrations is the step-in phenomenon. The push-out distances, 4−5 and 8−9 nm for solutions of 0.15 and 0.3 mM $C_{16}$TASal, respectively, correspond to about two- and four-layer thicknesses of $C_{16}$TASal, suggesting the push-out of adsorbed $C_{16}$TASal layers and/or inserted micelles. The remarkable pull-off phenomenon occurred, for all solutions examined here, on the outward process where the two surfaces in contact were pulled apart. The adhesion was strongest at 0.05 mM, which is below the cmc. This indicates the strong interaction between $C_{16}$TASal molecules, besides the interaction of $C_{16}$TASal with glass.

For aqueous solutions of various NaSal concentrations up to 1 M at a 0.15 mM $C_{16}$TASal, on the inward process, the electrostatic repulsive interaction at longer separations decreased with adding NaSal. This is due to the electrostatic shielding by salt excess. While the push-out at shorter separations was 3−5 nm for all solutions, the height of a force wall at 15−40 mN/m reached maximum at 0.01 M NaSal. During the outward process, the interlocking was minimized at 0.1 M NaSal. These tendencies, which are different from that of the electrostatic repulsion interaction, imply the strong cohesion between adsorbed $C_{16}$TASal layers.

**Acknowledgment.** This work was supported by a Grant-in-Aid for Scientific Research (A) (No. 05403012) by the Ministry of Education, Science and Culture in Japan. Author's are grateful to Mr. M. Jarnyk and H. Blemings of Anutech Pty Ltd. for their technical assistance.

LA990824Y